EPJ Web of Conferences **29**, 00022 (2012)
DOI: 10.1051/epjconf/20122900022

Synthesis, structural, magnetic and electrical properties of nominal $La_{0.67}Ba_{0.33-x}Na_xMnO_3$ ($0 \le x \le 0.33$) manganites

S. Hcini[a1], S. Zemni [1], M. Boudard [2], H. Rahmouni [3], M. Oumezzine [1]

[1]Laboratoire de Physico-chimie des Matériaux, Département de Physique, Faculté des Sciences de Monastir, 5019, Université de Monastir, Tunisie.
[2]Laboratoire des Matériaux et du Génie Physique (CNRS UMR 5628), Minatec Bâtiment INPG, parvis Louis Néel, BP 257, 38016 Grenoble Cedex 1, France.
[3]Laboratoire de Physique des matériaux et nanomatériaux appliqués à l'environnement, Faculté des Sciences de Gabes, Département de Physique, 6079, Université de Gabes, Tunisie.

Abstract. Complete nominal solid solutions $La_{0.67}Ba_{0.33-x}Na_xMnO_3$ ($0 \le x \le 0.33$) have been elaborated by ceramic route at 1200°C. ICPAES chemical analysis and XRD Rietveld structure refinement revealed that the nominal Na content is not achieved by our ceramic method. The chemical formula should be rather written as $La_\alpha Ba_\beta Na_\lambda MnO_{3-\delta}$ with a significantly lower Na content (λ), than the nominal one (x), and with a slight deficit (δ) in oxygen content, leading to the appearance of two minor secondary phases identified as Mn_3O_4 and $Na_{0.55}Mn_2O_4{\cdot}1.5H_2O$. Magnetization and electrical resistance vs. temperature show paramagnetic/semiconductor – ferromagnetic/metallic transitions with only a slight decrease in magnetic and electrical transition temperatures when Na content increases. Such amount of this decrease is not expected according to the nominal Na content giving a significant difference between nominal and experimental Mn^{4+}/Mn^{3+} ratios.

1 Introduction

The mixed-valence state perovskites, $Ln_{1-x}A_xMnO_3$ (Ln = rare earth, A = Ca, Sr, Ba ...) have taken considerable interest and have been extensively studied over the past fifteen years, following the discovery of colossal magnetoresistance (CMR) in these compounds [1]. Although the CMR was discovered for the first time in thin films of $La_{0.67}Ba_{0.33}MnO_3$ compound [1], the manganite system $La_{1-x}Ba_xMnO_3$ remains less studied than $La_{1-x}Ca_xMnO_3$ and $La_{1-x}Sr_xMnO_3$ homologous. Furthermore $La_{1-x}Ba_xMnO_3$ is one of the prototype materials with a large size difference ("mismatch" effect) between La^{3+} ($r_{La}{}^{3+}$=1.36Å) and Ba^{2+} ($r_{Ba}{}^{2+}$=1.61Å) [2]. The composition $La_{0.67}Ba_{0.33}MnO_3$ (x= 0.33) shows the highest Curie temperature (T_C= 350K [3]) in $La_{1-x}Ba_xMnO_3$ system. Recently we have studied the structural, magnetic and electrical properties of some manganites doped at Mn site by Ti, $La_{0.67}Ba_{0.33}Mn_{1-x}Ti_xO_3$ [4], or by Fe, $La_{0.67}Ba_{0.33}Mn_{1-x}Fe_xO_3$ [5], and we have showed for these compounds that the amount x= 0.1 of Ti or Fe is a limiting value of doping level above that we can't observe ferromagnetic/metallic - paramagnetic/semiconductor transitions and particularly with a Curie temperature value nearing the room temperature for x= 0.05 concentration, which is required for potential applications based on CMR and magnetocaloric effects. Another way to control the

[a] e-mail: hcini_sobhi@yahoo.fr

magnetic and electrical transitions temperatures is the substitution of barium by a monovalent cation such as sodium, with smaller radius, which reduces in particular the "mismatch" effect between La and Ba and may lead to significant changes in physical properties of the substituted compounds. Recently Das and Dey [6] have studied the magnetocaloric properties of nominal $La_{0.7}Ba_{0.3-z}Na_zMnO_3$ (z= 0.05, 0.1 and 0.15) manganites and have concluded that their materials are single phase rhombohedral $R\bar{3}c$, though the only X- ray diffraction pattern for z= 0.05, showed in their work, contains extra peaks of not identified secondary phases. Moreover, no quantitative chemical analysis of the prepared samples was presented and no special care was taken to reduce Na volatilisation. Besides there isn't a significant change of Curie temperature as a function of Na content in their work. These circumstances prompted us to examine the synthesis, quantitative chemical analysis, structural, magnetic and electrical properties of complete nominal solid solutions $La_{0.67}Ba_{0.33-x}Na_xMnO_3$ ($0 \leq x \leq 0.33$).

2 Experimental procedures

Samples were prepared by the traditional solid-state reaction method. Mixed powders of La_2O_3, $BaCO_3$, Na_2O_3 and MnO_2 precursors was heated at 800°C for 24h and then subsequently pulverized. The obtained powder was ground, pressed into pellets and sintered for 24h at 1000°C. This process was repeated at 1100°C and 1200°C, respectively, followed by furnace cooling in atmosphere. Powder X-ray diffraction (XRD) analyses were carried out with a "PANalytical X'Pert Pro" diffractometer with filtered (Ni filter) Cu radiation. Microstructure of specimens and their composition were studied by scanning electron microscopy (SEM) using a Philips XL30 microscope with an energy dispersive X-ray spectrometer, and with inductively coupled plasma atomic emission spectrometry (ICP-AES). Magnetizations (M) vs. temperature (T) and vs. magnetic field (H) were measured using extracting sample magnetometer. M(T) data were obtained at 0.05 Teslas, in 10 - 500 K temperature range. M(H) data were obtained at T= 50K, up to 10 Teslas. The electrical resistance vs. temperature was measured in 80 - 300K temperature range, using two electrical contacts done on samples having a disk shape with a diameter of 10mm and a thickness of about 2mm.

3 Results and discussion

Figure 1 exemplifies SEM micrographs of our samples. Below x= 0.1 Na amount, the micrographs show a unique chemical contrast corresponding to the manganite phase (see figure 1.a). For x= 0.15, 0.2 and 0.25 compositions SEM micrographs show a coexistence of two phases: a major primary phase with an homogeneous clear contrast corresponding to the manganite phase and a minor secondary phase with dark contrast identified as Hausmannite (Mn_3O_4) phase. Besides the two previously mentioned phases, SEM micrographs show a third phase (see figure 1.b) identified as Na-birnessite $Na_{0.55}Mn_2O_4 \cdot 1.5H_2O$ [7, 8] for x = 0.3 and 0.33. Results of ICPAES analysis indicate that the compositions of La, Ba and Mn are very close to the nominal ones, whereas Na content is significantly lower than the nominal one. Based on morphological characterization, EDX and XRD analyses we suggest that this loss of Na leads to lacunar manganite phase and to the formation of Mn_3O_4 and $Na_{0.55}Mn_2O_4 \cdot 1.5H_2O$ secondary phases, especially for higher Na amount. To quantify the proportion of the major manganite phase in our specimens we have reported in table 1 the results of ICPAES analysis corrected considering the presence of the Mn_3O_4 and $Na_{0.55}Mn_2O_4 \cdot 1.5H_2O$ minor secondary phases estimated by XRD quantitative analysis using the Rietveld [9] and EVA [10] methods.

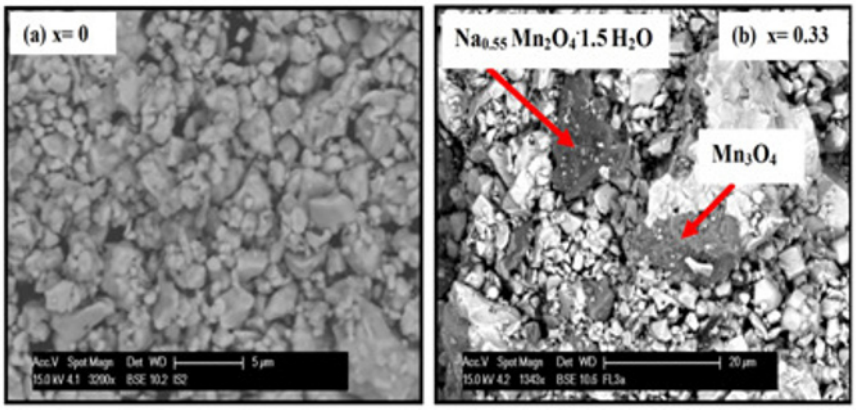

Fig. 1. SEM image (backscattered electron mode) of $La_{0.67}Ba_{0.33-x}Na_xMnO_3$ (x= 0, and 0.33) samples, showing that the undoped compound (Fig. 1.a) exhibits single phase while the nominal x= 0.33 compound (Fig. 1.b) exhibit two secondary phases besides the major manganite phase.

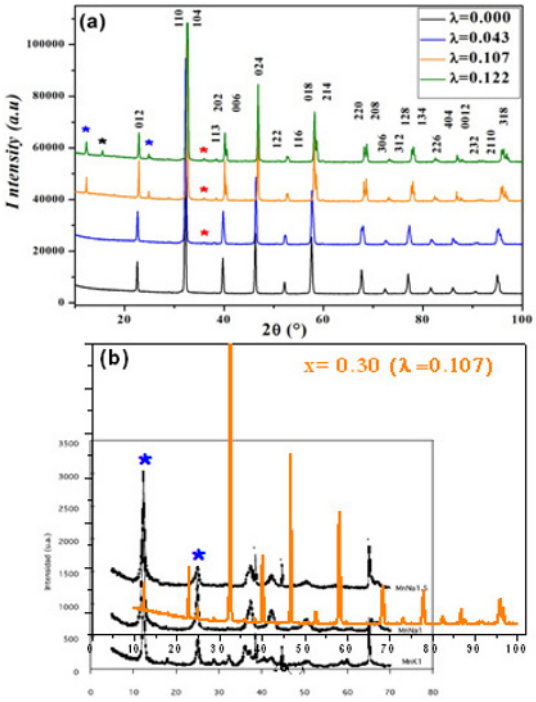

Fig. 2. (a) - X-ray diffraction patterns for $La_\alpha Ba_\beta Na_\lambda MnO_{3-\delta}$ ($0 \le \lambda \le 0.122$, only some spectrums are given). The asterisk denoted extra peaks of Mn_3O_4 (red color) and $Na_{0.55}Mn_2O_4{\cdot}1.5H_2O$ (blue color). All peaks of manganite phase are indexed in the hexagonal setting of the rhombohedral $R\bar{3}c$ symmetry. **(b)-** Extra peaks (indicated by asterisk with blue colour) in x=0.3 pattern match well with those of Birnessite $Na_{0.55}Mn_2O_4{\cdot}1.5H_2O$ (black colour) as published in [7, 8] works.

Figure 2.a presents the XRD patterns for solid solutions $La_\alpha Ba_\beta Na_\lambda MnO_{3-\delta}$ ($0 \le \lambda \le 0.122$) showing sharp and intense peaks corresponding to the major manganite phase. No impurity peaks were observed below $\lambda = 0.028$ (x=0.1) Na content, in agreement with SEM observations. However beyond that concentration the XRD patterns show at $2\theta = 36°$ a small peak (indicated by an asterisk in red color) corresponding to Hausmannite Mn_3O_4 phase. For higher Na content ($\lambda = 0.107$ and

0.122) this figure shows also two peaks at 2θ= 12.3° and 24.9° identified as $Na_{0.55}Mn_2O_4{\cdot}1.5H_2O$ peaks [7, 8]. Unfortunately our attempts are failed in the identification of the extra peak indicated by black asterisk in x=0.33 pattern. As shown in figure 2.b the presence of the two peaks indicated by blue asterisk in our XRD pattern (orange color) match well with those of $Na_{0.55}Mn_2O_4{\cdot}1.5H_2O$. Rietveld structure refinement revealed that the undoped compound and the doped one with 0.02 Na content exhibit a mixture of rhombohedral ($R\bar{3}c$, n°167) and orthorhombic (Imma, n°74) manganites phases. For all the other compounds the manganite phase exhibits only rhombohedral $R\bar{3}c$ symmetry.

Figure 3.a exemplifies the Rietveld refinement of XRD data for $La_{0.71}Ba_{0.15}Na_{0.076}MnO_{2.97}$ compound showing good agreement between observed and calculated profiles, if we consider the secondary Mn_3O_4 phase in the refinement.

In figure 3.b we gave XRD profiles of $La_{0.70}Ba_{0.25}Na_{0.05}MnO_3$ of Das and Dey [6] work in which we have added asterisk showing extra peaks matching well with those of Mn_3O_4 phase (compare Fig. 3.a and 3.b). These extra peaks are not considered for Rietveld refinement by Das and Dey [6]. On the other hand for x= 0.33 Na nominal content we compared in figure 4 our X-ray diagram (figure 4.a) with the one of $La_{0.67}Na_{0.33}MnO_3$ (LNMO) of Kalyana et al. [11] (figure 4.b). This comparison shows that our compound presents two extra peaks between 10° and 20°, which are not observed in the spectrum of Kalyana et al. [11], since such spectrum begins at 20°. However one can clearly see a third extra peak marked by asterisk (*) at 25° in the two diagrams. These suggestions give evidence that the nominal amount of Na in prepared manganites does not be achieved in [6, 11] works even the synthesis methods used by these authors differ from the one used by us.

Table 1. Atomic composition of the manganite phase as deduced from the results of ICPAES analyses corrected considering the two minor secondary, Mn_3O_4 and $Na_{0.55}Mn_2O_4{\cdot}1.5H_2O$ phases.

Na nominal content(x)	Mn_3O_4 (%at.)	$Na_{0.55}Mn_2O_4{\cdot}1.5H_2O$ (%at.)	$La_\alpha Ba_\beta Na_\lambda MnO_{3-\delta}$ manganite formula
0.00	0.0	0.0	$La_{0.67}Ba_{0.33}MnO_{3.02}$
0.05	0.0	0.0	$La_{0.65}Ba_{0.25}Na_{0.02}MnO_{2.9}$
0.10	2.0	0.0	$La_{0.72}Ba_{0.23}Na_{0.028}MnO_3$
0.15	2.5	0.0	$La_{0.70}Ba_{0.17}Na_{0.043}MnO_{2.98}$
0.20	2.5	0.0	$La_{0.71}Ba_{0.15}Na_{0.076}MnO_{2.97}$
0.25	3.0	0.0	$La_{0.73}Ba_{0.11}Na_{0.093}MnO_{2.96}$
0.30	3.0	2.0	$La_{0.73}Ba_{0.04}Na_{0.107}MnO_{2.98}$
0.33	4.0	3.0	$La_{0.77}Na_{0.122}MnO_{2.98}$

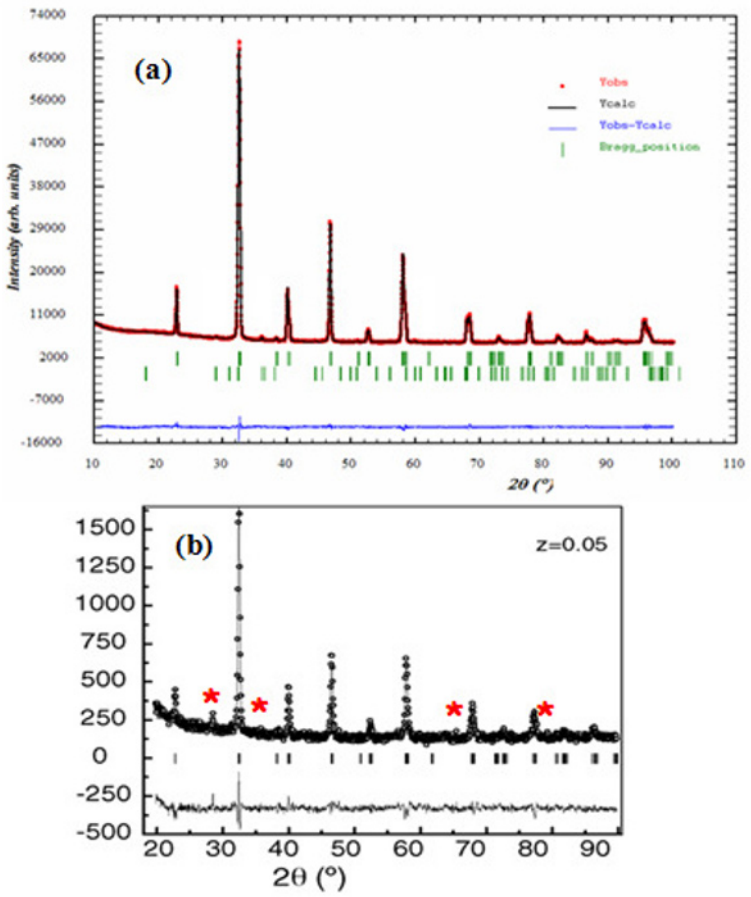

Fig. 3. (a)- Observed and calculated XRD profiles obtained by the Rietveld analysis. Their difference is represented at the bottom of the figure (blue solid line). The vertical ticks show the positions of the calculated Bragg reflections for $La_{0.71}Ba_{0.15}Na_{0.076}MnO_{2.97}$ (rhombohedral $R\bar{3}c$) and the minor Mn_3O_4 phase (tetragonal $I4_1/amd$). **(b)-** XRD profiles of $La_{0.70}Ba_{0.25}Na_{0.05}MnO_3$ of Das and Dey [6] work in which we have added asterisk showing extra peaks matching well with those of Mn_3O_4 phase (compare Fig. 3.a and 3.b).

Detailed results of Rietveld refinement for some of our samples are listed in Table 2. One can see in this table that cell volume, bond length $d_{Mn\text{-}O}$ and bond angle $\theta_{Mn\text{-}O\text{-}Mn}$ exhibit only a slight decrease, with the increase of Na, due to the small size of Na substituting the bigger Ba ion and especially to the important loss of Na. This is consistent with recent works [12, 13] showing that lattice parameters are mainly affected by the size effect of A perovskite site, inducing a significant change in the Mn–O–Mn bond angle.

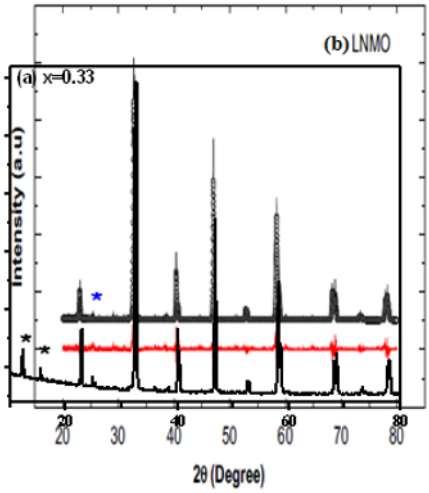

Fig. 4: Comparison of XRD patterns for x= 0.33 Na nominal content: **(a**) our $La_{0.67}Na_{0.33}MnO_3$ and **(b)** $La_{0.67}Na_{0.33}MnO_3$ (LNMO) of Kalyana et al. [11]

Table 2. Room temperature Rietveld refinement structural parameters for the rhombohedral $R\bar{3}c$ phase in $La_\alpha Ba_\beta Na_\lambda MnO_{3-\delta}$ ($0 \le \lambda \le 0.122$) manganites. The numbers in parentheses are estimated standard deviations for the last significant digit.

λ	**0**	**0.028**	**0.076**	**0.122**
Na nominal content (x)	**0**	**0.1**	**0.2**	**0.33**
Space group	$R\bar{3}c$			
a (Å)	5.5433 (2)	5.5285 (1)	5.5213 (1)	5.4885 (1)
c (Å)	13.4879 (2)	13.4714 (2)	13.4243 (2)	13.3157 (3)
V (Å^3)	358.93 (1)	356.58 (1)	354.41 (1)	347.38 (1)
La/Ba/Na B_{iso} (Å^2)	0.26 (6)	0.26 (1)	0.32 (2)	0.31 (2)
Mn B_{iso} (Å^2)	0.18 (1)	0.34 (3)	0.81 (2)	1.13 (3)
O x	0.5295 (3)	0.5354 (7)	0.5394 (6)	0.5408 (6)
O B_{iso} (Å^2)	1.14 (2)	1.02 (6)	0.98	1.218
$d_{(Mn)-O}$ (Å)	1.962 (1)	1.9611	1.9594 (4)	1.9473
$\theta_{(Mn-O-Mn)}$ (°)	170.6 (6)	168.52	167.25 (2)	166.7832
R_p (%)	1.41	1.29	1.4	1.44
R_{wp} (%)	1.82	1.66	1.94	2.22
R_{Bragg} (%)	2.38	1.1	2.5	4.04
R_F (%)	3.29	1.41	2.72	4.12
χ^2 (%)	1.55	1.55	2.30	3.14

Figure 5 shows magnetization vs. temperature, *M(T)*, at 0.05 Teslas applied magnetic field for all samples. A clear paramagnetic (PM) – ferromagnetic (FM) phase transition, corresponding to a sharp increase of *M(T)*, is observed in this figure. An estimation of the Curie temperature, T_C, for PM - FM phase transition was determined by the temperature where *dM(T)/dT* is minimum (see the a-inset of

figure 5). The T_C values obtained for all samples are listed in Table 3. It is observed that the compound λ= 0.028 (x= 0.1) has a Curie temperature T_C = 334K, practically the same of that of the undoped compound (λ= 0, T_C = 335K), then T_C decreases to 326K for λ= 0.043 (x= 0.15) and remains almost constant around 331K for λ= 0.076 and 0.093 (x= 0.20 and 0.25). This weak decrease of T_C with the increase of Na content is very consistent with the results of Das and Dey [6] work showing that T_C diminishes only by 5K when Na nominal content reaches z= 0.15. This result is a clear evidence that the chemical formula shouldn't be the same of the nominal one also in ref. [6]. The b – inset of figure 5 is an enlarged region of *M(T)* curves for temperatures below T_C. We can clearly see in that region a slight decrease in the magnitude of *M(T)* curves for the undoped compound (λ= 0) and for the doped one (λ= 0.028, x= 0.1), which should be ascribed to the contribution of the orthorhombic antiferromagnetic phase [14, 15]. Contrarily, beyond λ= 0.043, the magnetization exhibits a slight increase for all rhombohedral samples. Such increase is suddenly reinforced at 47K and below (see the b-inset of figure 5). This reinforcement is due to the contribution of the ferrimagnetic Mn_3O_4 secondary phase whose transition temperature is 46K as reported in ref. [16].

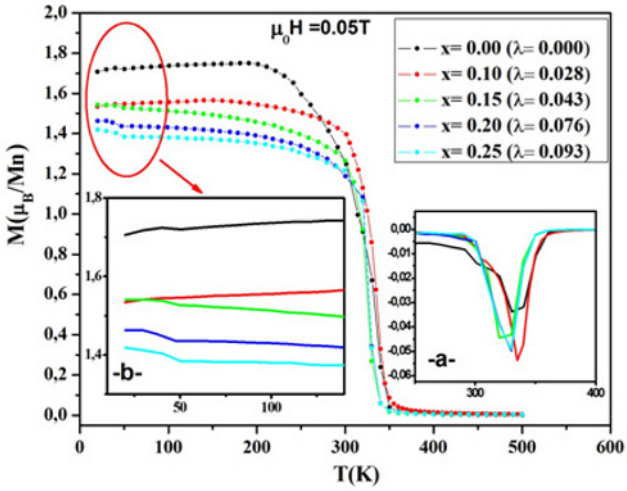

Fig. 5. Temperature dependence of the magnetization measured at magnetic field μ_0H = 0.05Teslas for $La_\alpha Ba_\beta Na_\lambda MnO_{3-\delta}$ ($0 \le \lambda \le 0.122$) manganites including, when present, the Mn_3O_4 secondary phase. The **a-** inset represents the *dM/dT* vs. *T* curve. The **b-** inset is an enlargement of data in low temperature region (below 150K)

Figure 6 shows the *M(H)* curves measured at 50K for samples with ($0 \le \lambda \le 0.093$). This temperature is selected just above the transition temperature (46K) of the ferrimagnetic phase Mn_3O_4 whose contribution to the magnetization is only relevant below this temperature. The *M(H)* curves exhibit a rapid increase with *H* at low magnetic fields, which suggests rearrangement of FM domains, whereas above 1 Tesla the magnetization is almost constant. This behaviour is consistent with the assumption of a FM state.

The observed and calculated magnetic saturation moments coincide reasonably (see table 3) when we consider the Mn^{4+}/Mn^{3+} ratio given by $La_\alpha Ba_\beta Na_\lambda MnO_{3-\delta}$ formula. But the difference between μ_s^{meas} and μ_s^{cal} becomes important if we use the Mn^{4+}/Mn^{3+} nominal ratio. This is a second indication that the nominal content of sodium is not achieved in our samples synthesized by ceramic method and also in some works through the literature. Hence, using usually the nominal chemical formula without doing quantitative chemical analyses leads to misinterpretation of properties of such manganites.

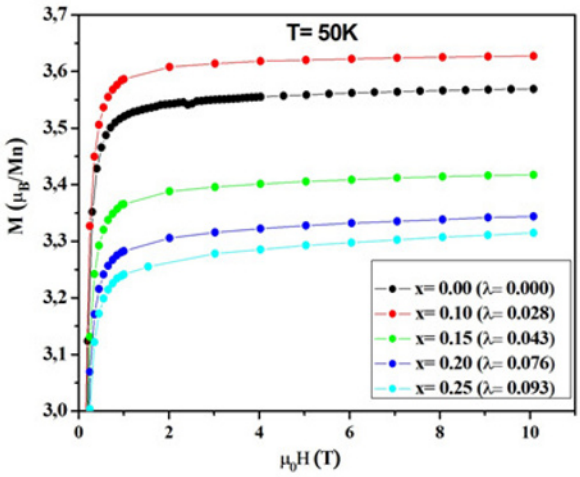

Fig. 6. Magnetization vs. magnetic field, *M(H),* measured at T= 50K for $La_\alpha Ba_\beta Na_\lambda MnO_{3-\delta}$ ($0 \le \lambda \le 0.122$) manganites.

Table 3: Magnetic and electrical parameters for $La_\alpha Ba_\beta Na_\lambda MnO_{3-\delta}$; μ_s^{cal}: theoretical saturation moment; μ_s^{meas}: experimental saturation moment deduced from the magnetization measured at 50K; T_C: Curie temperature; T_P: electrical transition temperature and R_{TP}: resistance peak.

Na nominal content (x)	λ	Mn^{3+}	Mn^{4+}	Mn^{4+}/Mn^{3+}	Nominal Mn^{4+}/Mn^{3+}	$\mu_S^{cal\,(a)}$ (μ_B/Mn)	μ_S^{meas} (μ_B/Mn)	T_C (K)	R_{TP} (Ω)	T_P (K)
0	0	0.63	0.37	0.587	0.493	3.63	3,57	335	5.45	265
0.05	0.02	0.67	0.33	0.493	0.613	-	-	-	-	-
0.10	0.028	0.65	0.35	0.538	0.754	3.65	3,63	334	6.59	263
0.15	0.043	0.53	0.47	0.886	0.923	3.53	3,42	326	7.46	240
0.20	0.076	0.57	0.43	0.754	1.128	3.57	3,34	331	7.55	250
0.25	0.093	0.59	0.41	0.695	1.381	3.59	3.32	331	9.26	251
0.30	0.107	0.42	0.58	1.381	1.703	-	-	-	37.04	243
0.33	0.122	0.47	0.53	1.128	1.941	-	-	-	27.86	238

[a] μ_s^{cal} values have been obtained by the following equation:

$$\mu_s^{cal}(\mu_B/Mn) = 2\mu_B(c_{Mn^{3+}} \times S_{Mn^{3+}} + c_{Mn^{4+}} \times S_{Mn^{4+}}) = 2\mu_B\left(c_{Mn^{3+}} \times \frac{1}{2} \times 4 + c_{Mn^{4+}} \times \frac{1}{2} \times 3\right)$$

where $c_{Mn^{3+}}$, $c_{Mn^{4+}}$ and $S_{Mn^{3+}}$, $S_{Mn^{4+}}$ are respectively the concentrations and the total spin of Mn^{3+} and Mn^{4+} ions.

The temperature dependence of resistance *R(T)* of the samples has been investigated over a temperature range 80–300 K and the behaviour is shown in figure 7. Using the sign of the temperature coefficient of resistance *dR/dT* as a criterion (*dR/dT* < 0) for a semiconductor behaviour and *dR/dT* > 0 for a metallic behaviour), all samples, except λ= 0.02 one, exhibit a metal-like behaviour at low-temperature ($T<T_P$) and a semiconductor-like one above T_P, where T_P is the temperature peak of resistance, as indicated by arrows in figure 7. The maximum of resistance, R_{TP}, and the electrical transition temperature, T_P, values obtained for all samples are listed in Table 3. In this table we note a slight increase in R_{TP} for samples with $0 \le \lambda \le 0.093$, while beyond λ= 0.093 (λ= 0.107 and 0.122), R_{TP} undergoes a sharp increase probably due to the contribution of the secondary $Na_{0.55}Mn_2O_4{\cdot}1.5H_2O$ phase. On the other hand T_P decreases from 265K for λ= 0 to 240K for λ=

0.043, then remains nearly constant (around 250K) for λ= 0.073 and 0.093, thereafter T_P decreases to 238K for λ= 0.122. One can notice that our T_P value for λ= 0.122 (x= 0.33) Na content is in good agreement with the reported one of Kalyana et al. [17] for $La_{0.67}Na_{0.33}MnO_3$ compound (T_P= 247K). This is a third indication that Na is partially reacted in LNMO compound synthesized by Kalyana et al. [11, 17]. We noted also that the T_P values of our specimens are lower than T_C values (see table 3). Such difference is often attributed to the grain boundary effects [18, 19]. Other studies suggest that the doping level in the A- site [20] as well as oxygen deficiency [19, 21] play an important role for the observed electrical behaviour.

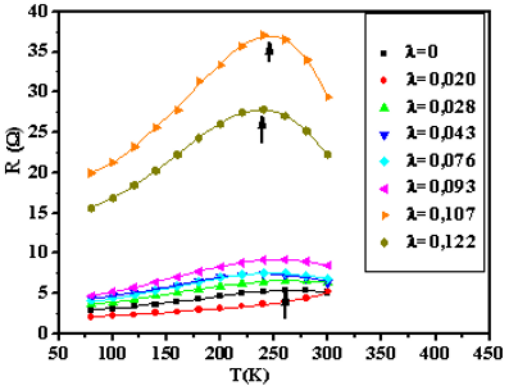

Fig. 7. Temperature dependence of the resistance *R(T)*, for $La_\alpha Ba_\beta Na_\lambda MnO_{3-\delta}$ ($0 \le \lambda \le 0.122$) manganites

4 Conclusion

Our results show that Na content (λ) in $La_\alpha Ba_\beta Na_\lambda MnO_{3-\delta}$ ($0 \le \lambda \le 0.122$) solid solutions obtained by chemical and XRD analyses, is significantly lower than the nominal one, x, in nominal complete solid solutions $La_{0.67}Ba_{0.33-x}Na_xMnO_3$ ($0 \le x \le 0.33$). The loss of Na induces lacunar manganites with a weak deficit (δ) in oxygen content and the appearance of minor secondary phases of Mn_3O_4 and $Na_{0.55}Mn_2O_4{\cdot}1.5H_2O$ for higher Na doping rate. The interpretation of magnetic and electrical properties was based on the Mn^{4+}/Mn^{3+} ratio determined according to $La_\alpha Ba_\beta Na_\lambda MnO_{3-\delta}$ formula. Such ratio is significantly different from the nominal one. Rietveld structure refinement revealed that compounds with λ= 0 and 0.02 exhibit mixed rhombohedral and orthorhombic phases but for λ≥ 0.028 the manganite phase exhibits single rhombohedral ($R\bar{3}c$) symmetry. Magnetic and electrical measurements show that these lacunar manganites exhibit ferromagnetic/metallic - paramagnetic/semiconductor transitions with a weak decrease in Curie temperature, T_C, and electrical transitions temperature, T_P, with increasing Na content. Our magnetic and electrical results are consistent with those of Das and Dey [6] and Kalyana et al. [17], which give a clear evidence that the nominal chemical formula of manganites does not be achieved in their work and secondary phases shouldn't be excluded. Hence, using usually the nominal chemical formula without doing quantitative chemical analyses leads to misinterpretation of properties of such manganites.

References

1. R. Von Helmolt, J. Wecker, B. Holzapfel, L. Schultz, K. Samwer, Phys. Rev. Lett. **71**, 2331 (1993)
2. R. D. Shannon, Acta Cryst. A **32**, 751-767 (1976)
3. C. Osthöver, P. Grünberg, R. R. Arnos, J. Magn. Magn. Mater. **177**, 854-855 (1998)
4. A. Gasmi, M. Boudard, S. Zemni, F. Hippert, M. Oumezzine, J. Phys. D: Appl. Phys. **42**, 225408 (2009)

5. M. Baazaoui, S. Zemni, M. Boudard, H. Rahmouni, A. Gasmi, A. Selmi, M. Oumezzine, Mater. Lett. **63**, 2167–2170 (2009)
6. S. Das, T. K. Dey, Mater. Chem. and Phys. **108**, 220–226 (2008)
7. V. Rives, M. Del Arco, O. Prieto, Bol. Soc. Esp. Ceram. V. **43**, 142-147 (2004)
8. A. Dias, Rodrigo G. Sá, Matheus C. Spitale, Maycon Athayde, Virgínia S.T. Ciminelli, Materials Research Bulletin **43**, 1528–1538 (2008)
9. H. M. Rietveld, J. Appl. Cryst. **2**, 65 (1969)
10. J. M. Le Meins, L. M. D. Cranswick, A. Le Bail, Results and conclusions of the Internet based "Search/match round robin 2002", , Powder Diffraction **18**, 106-113 (2003)
11. Y. Kalyana Lakshmi, G. Venkataiah, M. Vithal, P. Venugopal Reddy, Physica B **403**, 3059–3066 (2008)
12. G.Venkataiah, V. Parasad, P. V. Reddy, Solid State Commun. **141**, 73-78 (2007)
13. K. Bajaj, V. Bagwe, J. Jesudasan, P. Raychaudhuri, Solid state Commun. **138**, 549-552 (2006)
14. S. Chaffai, W. Boujelben, M. Ellouze, A. Cheikh-rouhou, J. C. Joubert, Physica B **321**, 74–78 (2002)
15. S. Savitha Pillai, P. N. Santhosh, N. Harish Kumar, P. John Thomas, F. Tuna, J. Phys.: Condens. Matter **21,** 195409 (2009)
16. K. Dwight, N. Menyux, Phys. Rev. **119**, 1470 - 1479 (1960)
17. Y. Kalyana Lakshmi, P. Venugopal Reddy, Journal of Alloys and Compounds **470**, 67–74 (2009)
18. S. Hcini, S. Zemni, A. Triki, H. Rahmouni, M. Boudard, Journal of Alloys and Compounds **509**, 1394–1400 (2011)
19. L. E. Hueso, F. Rivadulla, R. D. Sánchez, D. Caeiro, C. Jardón, C. Vázquez–Vázquez, J. Rivas, M. A. López–Quintela, Journal of Magnetism and Magnetic Materials **189**, 321-328 (1998)
20. O. Z. Yanchevskii, A. I. Tovstolytkin, O. I. V'yunov, D. A. Durilin, A. G. Belous. Inorganic Materials **40**, 744–750 (2004)
21. C. Shivakumara, M. B. Bellakki, Annigere S. Prakash, Nagsampagi, Y. Vasanthacharya, J. Am. Ceram. Soc. **90**, 3852–3858 (2007).